Growth dynamics of ultrasmooth hydrogenated amorphous carbon films

J. G. Buijnsters, M. Camero, and L. Vázquez*

Instituto de Ciencia de Materiales de Madrid (CSIC), C\Sor Juana Inés de la Cruz No. 3, 28049 Madrid, Spain

(Received 6 April 2006; revised manuscript received 2 August 2006; published 13 October 2006)

We have studied the growth dynamics of ultrasmooth hydrogenated amorphous carbon films deposited on silicon substrates by electron cyclotron resonance chemical vapor deposition from argon/methane gas mixtures applying a high negative external bias. The surface morphology of films deposited for different growth times under the same experimental conditions was analyzed by atomic force microscopy. Our analysis leads to values of the growth, roughness, and coarsening exponents of 0, 0.1, and 0.5, respectively. As it has been recently proposed that the growth dynamics of amorphous films by ion-assisted methods should obey the Edwards-Wilkinson (EW) growth mode, we have analyzed the compatibility of our data with this model. Our analysis indicates that, although the scaling data could be interpreted in terms of the EW model, the relative large data error bars and the film ultrasmoothness preclude the unambiguous assessment of the EW growth mode for our film growth evolution. In our system, the interplay of shadowing, physical sputtering and enhanced surface mobility ion-induced effects contribute likely to the leveling and final ultrasmoothness of the film surface.

I. INTRODUCTION

The unique combination of properties of diamondlike carbon (DLC) films has stimulated great interest in the deposition and application of these films over the last decades. Their high wear resistance, low friction coefficient, chemical inertness, surface smoothness, and biocompatibility already led to their use as protective coatings in numerous devices. In particular, surface smoothness becomes a crucial property for developing protective coatings for magnetic storage devices and low friction coatings.[1] Therefore, over the last years special attention has been paid to the production of ultrasmooth DLC films. Along with this applied effort, there is an increasing interest in understanding the mechanisms leading to such ultrasmooth films. This study implies the morphological characterization of the growth dynamics under the framework of the dynamic scaling theory.[2–4] The magnitude most commonly employed to characterize statistically the surface morphology for a given growing system with size L and observed at time t is the roughness, $\sigma(L,t)$, also known as the interface width. Representing the local surface height at position $\mathbf{r}$ and time t by the function $h(\mathbf{r},t)$, the interface width is defined as the mean square deviation of the local height with respect to the mean height $\langle h \rangle$ (Ref. [2])

$$\sigma(L,t) = \langle [h(\mathbf{r},t) - \langle h \rangle]^2 \rangle_{\mathbf{r}}^{0.5}, \qquad (1)$$

where the operator $\langle \cdots \rangle_{\mathbf{r}}$ represents the average over all r in a system of size L. In the dynamic scaling theory the surface roughness follows the Family-Vicsek dynamic scaling[3]

$$\sigma(L,t) = L^{\alpha} f(t/L^{z}), \qquad (2)$$

where $f(x)$ is a function that scales as x^{β} for $x \ll 1$ and is a constant for $x \gg 1$. The exponents α, β, and z are usually known as the roughness, growth and dynamic exponents, respectively. They are characteristic of the mechanism governing the system growth dynamics, and related between them by the expression $z = \alpha/\beta$. The roughness exponent describes the lateral correlations of the surface roughness while the growth exponent describes the surface roughening process in time through the powerlike behavior $\sigma \propto t^{\beta}$. Finally, $1/z$ is known as the coarsening exponent describing the coarsening process of the typical lateral correlation length of the system, ξ.

In order to characterize the surface roughness correlations different functions can be used.[2,4] In this work, we have employed: (a) The structure factor or power spectral density (PSD) defined as $\mathrm{PSD}(k,t) = \langle H(k,t)H(-k,t) \rangle$, where $H(k,t)$ is the Fourier transform of the surface height in a system of lateral size L, k being the spatial frequency in the reciprocal space; (b) the height-height correlation function defined as $G_2(r,t) = \{\langle [h(\mathbf{r}+\mathbf{r}',t) - h(\mathbf{r}',t)]^2 \rangle\}^{0.5}$.[2]

We have focused our research on the study under this framework of the growth dynamics of hydrogenated amorphous carbon (a-C:H) films, which have been produced by electron cyclotron resonance chemical vapor deposition (ECR-CVD) from a methane/argon gas mixture on silicon substrates. This type of films is attractive, for instance, in magnetic storage technology where a slightly hydrogen-rich surface is desired because the lubricant work prefers a slightly hydrogen-rich surface.[1] In addition, the ECR-CVD technique allows film deposition at low temperatures with high growth rates due to the relative highly ionized plasma beam and it does not intrinsically produce particles, such as in filtered cathodic vacuum arc (FCVA). Besides, the addition of argon to the methane ECR plasma results in increased hydrocarbon ion concentrations at the depositing surface via gas chemistry selection.[5] Moreover, the film surface bombardment by relatively heavy Ar^+ ions leads to increased dangling bond densities at the exposed growth surface.

The films have been deposited at different external bias and their corresponding film morphology has been studied by atomic force microscopy (AFM). From these analyses we have determined the best bias conditions to produce ultrasmooth a-C:H films and we have addressed the investigation on the smoothening mechanisms involved.

II. EXPERIMENTAL

The a-C:H films were grown by ECR-CVD (ASTEX, mod. AX4500) in a two-zone vacuum chamber[6] operating
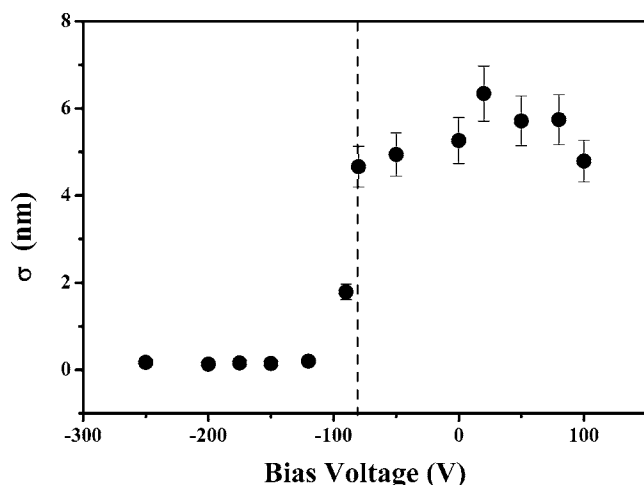
FIG. 1. Plot of σ, obtained from 1×1 μm^2 AFM images, of the a-C:H films grown for 1 h as a function of the external applied bias in which the two roughness regimes are observed. The vertical dashed line indicates the threshold bias from which physical sputtering effects are expected.

with a 2.45 GHz microwave plasma source at $208-210$ W input power. Gas mixtures of methane/argon (15 sccm/ 35 sccm) were applied keeping the operating pressure at 1.1×10^{-2} Torr. P-type silicon (100) substrates (280 μm thickness, double-side polished), with a surface roughness of $0.09-0.1$ nm, were used. A dc bias varying from -300 to $+100$ V was applied to the silicon substrates while no intentional heating was employed. The growth rate was close to 0.22 nm/s except for the samples grown at -75 to -150 V, in which a slightly higher growth rate was observed. It is important to mention that the temperature reached at the end of the deposition process was always lower than 115 °C as measured by a thermocouple attached to the substrate holder. Under these conditions, all films were amorphous as proved by micro-structural analysis.

The AFM characterization was performed with Nanoscope IIIa (Veeco) equipment operating in tapping mode with silicon cantilevers (nominal radius of 10 nm). Due to the extreme flatness of the studied surface, each a-C:H film was measured with a new fresh tip, which was afterwards used to measure the silicon substrate. Only those data obtained with tips that gave reliable roughness values of the substrate were used in the analysis. Regarding the roughness scaling analysis, we measured at least three films for each growth condition. For each sample, we measured by AFM at four different locations. Thus, the error bars depicted in the figures involving roughness data result from the deviations in these measurements. The graphs displaying power spectral density (PSD) and height-height correlation functions as well as those depicting the dependence of roughness with the length scale do not show error bars for sake of clarity but they are the average of the different realizations. As the correlation length was estimated from the PSD curves, its corresponding error bar was estimated from the sampling statistics of the PSD data.
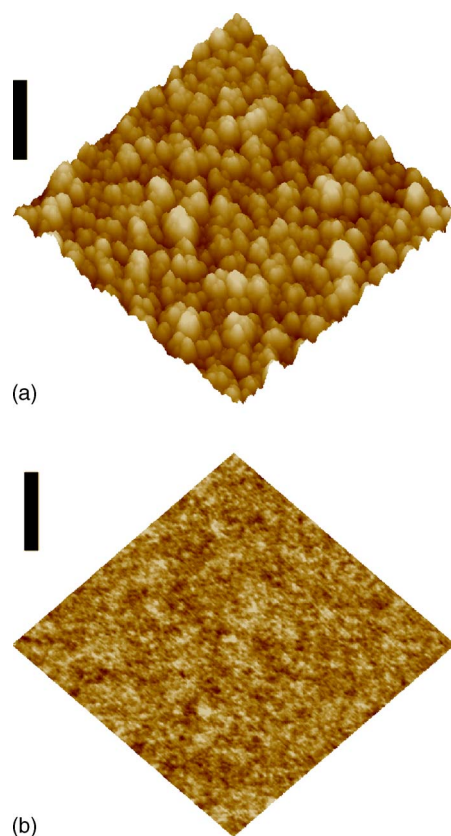

(a)

(b)

FIG. 2. (Color online) 1×1 μm^2 tapping mode AFM images of the a-C:H films grown for 1 h: (a) without external bias; (b) with an external bias of -200 V. The vertical bar represents 80 nm.

III. RESULTS AND DISCUSSION

A. Influence of substrate bias on film morphology

The surface roughness, σ, obtained from AFM images, versus the applied bias during deposition is displayed in Fig. 1. Indisputably, there are two main regimes separated by a sharp transition at ~ -80 V. It is worth commenting that this bias crossover value is in the range of the threshold ion energy, in the $80-100$ eV range, reported for the formation of hard carbon films by various techniques.[7,8] The first regime, running from -80 V up to positive bias, is characterized by a relatively large film roughness. For the second one, for high negative bias, σ is extremely low, in the $0.1-0.16$ nm range. In our case, the ultrasmooth films did prove to be hard (~ 18 GPa) and wear resistant ($\sim 1 \times 10^{-7}$ mm^3/Nm) and displayed a hydrogen content of about 30 at. % while the films grown without bias had an hydrogen content of about 55 at. % The surface morphology of a film deposited at 0 V for 1 h [Fig. 2(a)] is cauliflowerlike since large protuberances, which contain also smaller granular structures, are observed. This kind of morphology is obtained for all the films belonging to the high roughness regime. In contrast, the films obtained in the low roughness regime show a flat and featureless morphology [Fig. 2(b)]. In this case, the film roughness is less than 0.2 nm with maximum peak to valley height values of 1.2 nm.
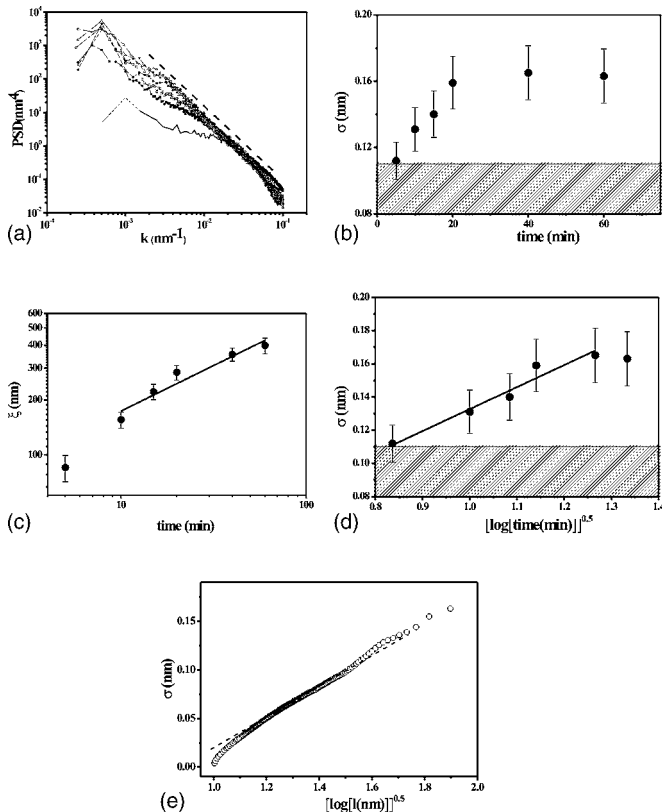
FIG. 3. (a) PSD curves corresponding to the silicon surface (solid line) and the films grown at −200 V for 5 (-■-), 10 (-□-), 15 (-●-), 20 (-*-), 40 (-○-), and 60 (-△-) min. The dashed line corresponds to a slope of −2.2. (b) Plot of σ vs t for films grown with an external bias of −200 V. The shadowed bottom region corresponds to the range of roughness values measured on the silicon substrate. (c) Plot of ξ, obtained from the PSD curves, versus the growth time. The solid line corresponds to the best fitting obeying the $\xi \propto t^{0.5}$ relationship for $t > 5$ min. (d) Plot of σ vs $(\log t)^{0.5}$ for the same films of (b). The points, from left to right, correspond to deposition times of 5, 10, 15, 20, 40, and 60 min. The solid line is the best fit following the dependence $\sigma \propto (\log t)^{0.5}$, which is a straight line in this type of display. (e) Plot of σ vs $(\log l)^{0.5}$ for the thickest film grown at −200 V, i.e., deposited for 1 h. The dashed line indicates the range in which $\sigma \propto (\log l)^{0.5}$.

B. Scaling analysis of ultrasmooth films

In order to better characterize this smoothening process we have analyzed the evolution of the film surface morphology as a function of deposition time when an external bias of −200 V is applied. In all these cases, the films present a smooth morphology, similar to that depicted in Fig. 2(b). For deposition times spanning from just 5 min up to 1 h the film roughness was always extremely low: in the 0.1–0.16 nm range.

We have addressed the analysis of these data under the framework of the dynamic scaling theory in order to obtain the values of exponents α, β, and $1/z$. In principle, a suitable method to obtain the α exponent value is from the PSD curves, that is, in the reciprocal space, in logarithmic scales.[9] Accordingly, we show in Fig. 3(a) the PSD curves corresponding to the silicon substrate and the a-C:H films for the

different growth times. The PSD curves present a linear behavior, in the logarithmic representation, which extends to smaller k values (i.e., larger length scales) as the growth time increases. The slope of the linear behavior of the PSD curves is indicated by the dashed line, and equals −2.2, which implies $\alpha \approx 0.1$. It should be noted that for the shorter growth times and the smaller k values, the PSD curves tend to run parallel to the PSD curve corresponding to the silicon substrate. This behavior indicates that for large length scales the film morphology is dominated by the substrate morphology. Also, note that for the smallest k values (i.e., largest length scales) all the PSD curves increase displaying a maximum. This feature could also come from the substrate morphology or/and could be influenced by the poorer data sampling statistics at the smallest k values.

The value of the slope (i.e., −2.2) of the linear regime of the PSD curves displayed in logarithmic scales allows us to discard different possible mechanisms as the cause of the film surface ultrasmoothness. Thus, surface[2] and bulk diffusion[10] predict a slope of the PSD of −4 and −3, respectively. Additionally, surface or bulk viscous flow effects[11] imply a slope of −4 and −1, respectively. As these values differ largely from that obtained in our work, we can discard all these phenomena as the origin of the observed ultrasmoothness.

In order to further characterize the growth dynamics of our system, we have determined the value of β. Thus, in Fig. 3(b) we display the evolution of the surface roughness with the growth time. In all cases, the roughness values are in the 0.1–0.16 nm range. This behavior implies $\beta \approx 0$.

We have also analyzed the dependence of the lateral correlation length, ξ, with the growth time. The value of ξ for each growth time was obtained from the corresponding PSD curve as it corresponds to the inverse of the smallest k value on the linear regime (in logarithmic representation). The plot of the change of this length with the growth time is shown in Fig. 3(c). The straight line corresponds to the best fit following the $\xi \propto t^{0.5}$ scaling behavior for $t > 5$ min, which implies $1/z \approx 0.5$. Within the experimental errors, this behavior is consistent with the experimental data for $t > 5$ min. Also, it is worth noting that the value of ξ is 5–6 times larger than that reported for tetrahedral amorphous carbon, ta-C, films grown by FCVA and high current arc (HCA).[12] This difference could be due to both the larger film thickness of the a-C:H films, and the higher average ion energy in the ECR plasma as at higher ion energies the extent of the lateral smoothening induced by the ion impact is larger.[13]

The values obtained for the scaling exponents, $\alpha \approx 0.1$, $\beta \approx 0$, and $1/z \approx 0.5$ are indeed consistent with the observed ultrasmoothness. Recently, Moseler *et al.* have proposed[13] that the growth of amorphous films in which ion-assisted processes are employed obeys the Edwards-Wilkinson (EW) growth model.[14] Since our films are produced by an ion-assisted process (ECR-CVD) and they are amorphous, we have contrasted our experimental data with the behavior expected for the EW model.

The EW continuous growth equation for the local surface evolution has the following expression:

$$\partial h/\partial t = \nu \nabla^2 h(\mathbf{r},t) + \eta(\mathbf{r},t), \tag{3}$$

where, ν is a positive constant and η represents the random character of the arrival of the depositing particles to the interface. This equation is related to evaporation/condensation processes since those regions located at surface depressions (i.e., $\nabla^2 h > 0$, local positive surface curvatures) grow faster than those located at surface protrusions (i.e., $\nabla^2 h < 0$, local negative surface curvatures). In principle, these phenomena are very unlikely under our current growth conditions. However, it has been reported that this kind of growth can result from the interplay of different growth phenomena.[13,15] Thus, we have further analyzed the dependence of the surface roughness in order to unambiguously determine whether the EW model is consistent or not with the experimental behavior. Edwards and Wilkinson showed[14] that for a $2+1$ system as ours the EW equation implies that

$$\sigma \sim [\log(t)]^{0.5} \tag{4}$$

for short times, and

$$\sigma \sim [\log(l)]^{0.5} \tag{5}$$

for long times.

In order to check if our system follows these dependencies, we have first plotted the σ values versus $(\log t)^{0.5}$ in Fig. 3(d). We observe that for the $5-30$ min growth time range, before saturation, the experimental behavior is consistent with the relationship $\sigma \propto (\log t)^{0.5}$ as a linear regime is clearly observed, which is consistent with an EW scaling.[2,14,16] However, we should note that the unambiguous assessment of the $(\log t)^{0.5}$ dependence becomes difficult because of the extreme surface smoothness and, therefore, of the relatively large error bars. In addition, it should be noted that usually the experimental assessment of this dependence becomes very difficult.[17]

Thus, we have also analyzed the dependence of the surface roughness with the square root of the logarithm of the length for the thickest film (i.e., longest deposition time). The result is shown in Fig. 3(e). Clearly, in the representation of σ versus $[\log(l)]^{0.5}$, a wide linear region is observed, which is expected for the EW growth mode. However, the roughness does not saturate at larger length scales beyond this region, as it should be expected, but increases. This feature is associated with the corresponding increase in the PSD curve [Fig. 3(a)] for small k values, which can be due to the influence of the substrate morphology as discussed above.

In principle, these results indicate that the growth dynamics of the a-C:H films deposited by ECR-CVD at a external bias of -200 V could be interpreted in terms of the EW growth model. However, the relative large error bars of the roughness data [Fig. 3(d)] and the possible influence of the substrate morphology at large length scales [Fig. 3(e)], which become relevant for such ultrasmooth films, preclude the unambiguous assessment of the EW growth model for our system.

C. Experiment on ion-induced smoothening effects

In order to obtain further insight into the smoothening mechanisms leading to the ultrasmooth films at high bias values, we have designed the following experiment. We have grown two polymeric a-C:H films without external bias for 30 min (film A) and 60 min (film B), respectively. In addition, on a parallel film A we have continued the film growth for 30 min more under the same conditions but at a negative bias of -200 V (film C). The corresponding surface morphologies measured by AFM are displayed in Figs. 4(a)–4(c), respectively. Also, typical surface profiles corresponding to the dashed lines depicted in Figs. 4(a)–4(c) are shown in Fig. 4(d). From these data, it is evident that films A and B have a characteristic cauliflowerlike rough surface morphology. As the AFM images suggest and Fig. 4(d) confirms, both the surface roughness and the average feature (i.e., cauliflower) size are larger for film B than for film A. For biases more positive than -70 V, as it is the case of films A and B, the polymeric film surface is rough due to the random arrival of relatively low energetic depositing species. It is known[18] that non-normal incidence trajectories are inherent within CVD processes. Thus, the incoming particles impinge more likely at the surface protrusions rather than at the surface valleys or depressions leading to the development of growth instabilities, which is consistent with a scenario in which shadowing effects operate.[19,20] In contrast, Fig. 4(c) indicates that film C has a quite different surface morphology, more compact and with a smaller average lateral size of the surface features. This is confirmed in Fig. 4(d) that shows the corresponding surface profile. This profile, compared with those of films A and B, is leveled off in a great extent. Additionally, the surface profile shows that the lateral size of the characteristic surface features has been reduced. Thus, the surface morphology has been clearly smoothed.

From the comparison of the respective PSD curves, shown in Fig. 4(e), we observe the overlapping of the three PSD curves in a linear region, which is indicated by the dashed line in the logarithmic plot, for large k values (i.e., short length scales). As commented above, the smallest k value of the linear regime (in the logarithm plot) of each PSD corresponds to the typical lateral correlation length of the film, ξ_g. In the case of samples A and B this distance corresponds to the average size of the cauliflowerlike structures while for sample C it is related to the average film grain size. Thus, the crossover k values of films A, B, and C correspond to ξ_g values of ≈ 38, ≈ 59, and ≈ 25 nm, respectively. In addition, for the PSD curves of samples A and B the respective K_A and K_B values are close to the horizontal part of the curves at small k values for which the surface is uncorrelated. This fact implies that the film roughness is mainly determined by the contribution of the cauliflowerlike structures. In contrast, for sample C there is still a clear correlated regime for $k < K_C$, which indicates that the film roughness has contributions from the grain morphology as well as from the height fluctuations between grains (i.e., for lengths larger than the ξ_g). It is worth noting that the PSD of film C is below those of films A and B just for $k < K_C$, which implies that the reduction in surface roughness takes place for $l > \xi_g$. Thus, the ion-induced smoothening process takes place through the reduction of ξ_g and the leveling of the surface for $l > \xi_g$. In the inset of Fig. 4(e) we show the height-height correlation function of the AFM images corresponding to the same films of Fig. 4(e). Basically, the same
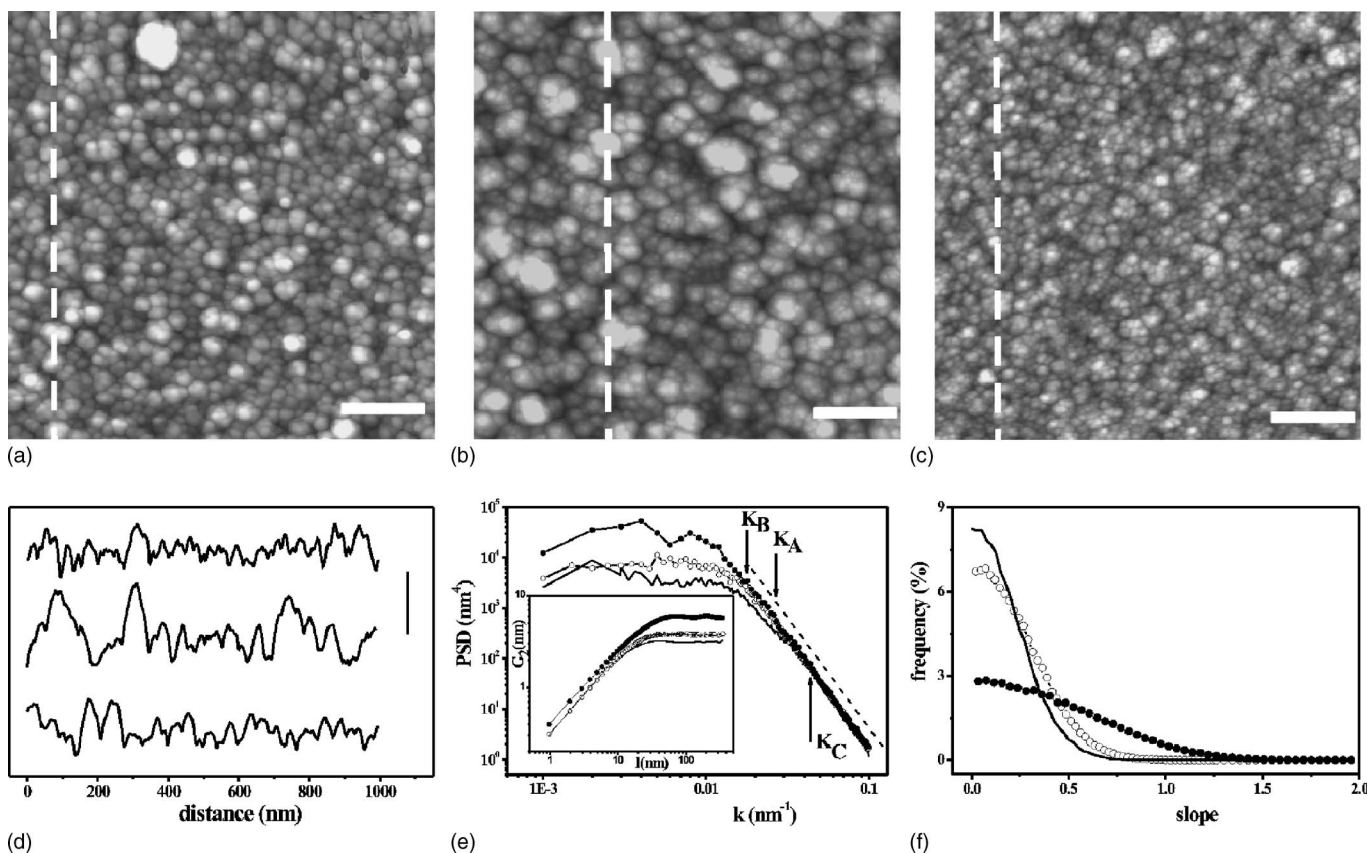
FIG. 4. 1×1 μm^2 tapping mode AFM images of the a-C:H films: (a) A, (b) B, and (c) C. In all cases the horizontal bar indicates 200 nm. The dashed lines correspond to the surface profiles displayed in (d). (d) Typical surface profiles of the films A (bottom profile), B (middle profile), and C (top profile). The vertical bar indicates 10 nm. (e) PSD curves corresponding to films A (-○-), B (-●-), and C (solid line). K_A, K_B, and K_C indicate the crossover points associated with the corresponding film grain or cauliflowerlike structure sizes. The dashed line indicates the linear region in the logarithmic plot. Inset: Height-height correlation functions corresponding to the same films A, B, and C of (e). (f) Surface slope normalized distribution for films A (-○-), B (-●-), and C (solid line).

behavior is observed since the three functions run parallel for small length scales and that one corresponding to film C is below those of films A and B for large length scales. This figure shows a new feature, namely that the $G_2(r,t)$ function is shifted upwards for the cauliflower growth conditions as the deposition time increases as can be seen by comparing the curves of samples A and B. This vertical shift is a clear indication that the growth under these conditions is unstable and that the local surface slopes increase.[21] This behavior agrees with that observed in Fig. 4(f), in which the surface slope distributions of films A, B, and C are displayed. Clearly, the comparison of the distributions of films A and B implies that the growth without bias causes an increment of the higher slopes, in detriment of the low ones, as the growth proceeds. This trend is reversed when a higher bias is applied (film C) since the high slope contribution is drastically reduced and the relative weight of the low slopes is even higher than that found initially for film A. This behavior is a consequence of the smoothening processes operating when the growth is assisted by relatively high-energy ions.

IV. DISCUSSION

In order to better understand the physical mechanisms operating during the growth of our ultrasmooth a-C:H films, it is worth comparing our results with the scarce growth scaling analysis on similar systems as well as to analyze the most relevant growth processes that take place in our system.

Regarding previous studies on growth dynamics under the dynamic scaling theory framework of ultrasmooth amorphous carbon films, the main system studied has been ultrasmooth ta-C films grown by FCVA (Refs. 12 and 13) and HCA.[12] For the HCA films, which were grown on ultrasmooth silicon substrates (rms roughness ~0.1 nm), the surface film roughness was ~0.12 nm for all the deposition times. This behavior is quite similar to ours and implies $\beta \approx 0$. In the case of the FCVA ta-C films, which were grown on a slightly rougher Si(100) substrate (rms roughness ~0.2 nm), as the deposition time increased the surface roughness initially decreased until a constant value ~0.11 nm was reached. In this constant regime, $\beta \approx 0$ was obtained. In a first study of both systems,[12] based on the analysis of the height-height correlation function, the scaling analysis led to scaling exponents, $\alpha \approx 0.39$ and $\beta \approx 0$, that were not explained by any of the existing models.[12] In that case the ultrasmoothness was explained as the consequence of short thermal spikes by ion impact accompanied by a reduction of the local interface curvature.[12] In a second study of the FCVA system, based on the fitting by the EW model of the PSD *in a linear representation*, the growth dynamics was

considered to be consistent with it.[13] There, it was proposed, from molecular dynamics simulations, that the existence of an ion-induced downhill current of material leads to a local growth rate dependence on the local surface curvature, which is associated to the EW growth mode. Moreover, this mechanism is also predicted[13] to govern the film growth for other amorphous systems, in which ion-assisted processes are employed, such as our system and the HCA *ta*-C one. In this sense, we can comment that our PSD curves were similarly well fitted in a linear representation (not shown) by the EW model.

As we have already explained, we cannot identify our growth dynamics as EW. However, our results qualitatively agree with some of the behaviors predicted in the work of Moseler *et al.*[13] Thus, the observed dependence (Fig. 1) of the surface roughness on the ion energy agrees qualitatively with that predicted in this model, and is observed for *ta*-C FCVA films. In that study, for increasing ion energies up to 100 eV the surface roughness decreases while for ion energies equal or larger than 100 eV, it saturates at the minimum attained value. This behavior was explained by the increase of ion induced surface currents with the ion energy until subplantation effects at deeper lengths start to operate at ion energies of ≈ 100 eV. In our case, for biases more negative than -70 V the surface roughness decreases continuously until for ion energies equal or larger than 150 eV the surface roughness is saturated and it is not further reduced for higher ion energies.

At this point, it is convenient to discuss the main processes involved in the *a*-C:H growth by ECR-CVD that can lead to the observed film ultrasmoothness. The *a*-C:H film deposition by ECR-CVD from a methane/Ar plasma is a complex system.[22] In fact, the deposition process is the result of several factors such as plasma chemistry, gas-surface interaction, surface chemistry, and etching and bombarding effects. In our system, the key role of the external bias value and, therefore, of the ion energy on the film morphology is evidenced in Figs. 1 and 2. In our case, the magnitude of the bias defines the energy of the ions, 70% argon and 30% hydrocarbon species, impinging on the growing film surface. While the former do not contribute to the film growth, the latter indeed are finally incorporated into the growing film. Thus, we focus on the different effects induced on the growing film by the impinging of the energetic ions. (i) First, the protruding regions of the growing film surface will receive more depositing species[18] and incoming ions than those located at depressions or lower heights. (ii) The ion bombardment of the film surface increases the sticking coefficient of the impinging radical growth precursors through the creation of dangling bonds on the surface.[23] The energy required for these processes being relatively low since it is close to 2 eV.[24] (iii) For the growth of ultrasmooth hydrogenated amorphous silicon, *a*-Si:H, films deposited by plasma assisted CVD, which is quite similar to ours, it has been reported that ion bombardment induces an enhanced mobility of the precursor species weakly bound to the film surface.[20] Thus, we can expect that a similar process takes place in our system. (iv) For the bias condition for which ultrasmooth films are obtained, the impinging ions have energies higher than the threshold value required for physical sputtering, which is in the range of 80 eV.[24]

The first effect will cause that shadowing effects for both the deposition of incoming species and the ion bombardment may arise. This was indeed the case for the low bias growth conditions where rough cauliflowerlike surface film morphologies (i.e., unstable growth mode) were obtained. At higher bias values, these shadowing effects together with the ion-induced increase of the sticking probability should lead to an even enhanced unstable growth because the particles that reach mainly the protruding regions should incorporate with high probability to the film. The observed behavior implies that the interplay of just these two effects does not govern the film growth. The third effect, the ion-induced enhanced mobility of precursor species on the film surface, can contribute to the ultrasmoothness of the growing film through the suppression of surface growth instabilities, as it has been demonstrated for the growth of *a*-Si:H films by plasma assisted CVD.[20] This enhanced precursor surface mobility implies a homogeneous distribution on the growing interface of the species that contribute to the film growth. For such system $\beta \approx 0$ was found. Moreover, it has been shown that for DLC films produced by the deposition of carbon clusters the mobility of surface atoms increases with the cluster incident energy.[25] In particular, for energies in the 60 eV range, this enhanced mobility contributes to the production of smooth DLC films. Finally, if we consider the fourth effect, the physical sputtering of the film by the energetic ions, the growth scenario can change due to the shadowing effects. Under these conditions, the impinging atoms will erode easier the surface protrusions inducing a leveling of the growing surface. Thus, when etching processes occur within a shadowing geometry or for diffusion (i.e., transport) limited processes, the surface morphology tends to be smoothed.[26–28] The experiment of Fig. 4 is consistent with this explanation since it is clear that the smoothening of the rough cauliflower film at high bias suppresses the larger protrusions and surface slopes leading to an evident leveling of the surface, which agrees with a preferential sputtering of the higher surface regions. Moreover, Fig. 1 shows clearly that the sharp transition from the rough unstable growth mode, at low bias values, to the ultrasmooth one takes place at bias values slightly higher than the threshold value of 80 eV for physical sputtering. It is worth noting that there are also chemical sputtering effects in the ion-assisted growth of *a*-C:H films.[29] However, these processes usually take place already at ion energies of 20–30 eV or even lower values. This energy range is quite lower than the bias values for which ultrasmooth film growth is observed (Fig. 1). Accordingly, we can assume that physical sputtering effects are more relevant for the film surface morphology. Under this growth scenario, the simultaneous operation of shadowing effects, physical sputtering and the enhanced precursor surface mobility can lead to the observed ultrasmoothness of our *a*-C:H films.

V. CONCLUSIONS

Our results clearly show that the ion energy plays a fundamental role in the production of ultrasmooth *a*-C:H films by ECR-CVD by smoothening the surface morphology in the

nanometer range and by suppressing the local high surface slopes. In addition, the a-C:H film ultrasmoothness is associated with a high film hardness and wear resistance. This correlation suggests that at energies higher than 80 eV the ion bombardment affects simultaneously the surface morphology and the internal bonding structure. Our analysis shows that the film growth under relatively high bias conditions leads to ultrasmooth surfaces with $\alpha \approx 0.1$, $\beta \approx 0$, and $1/z \approx 0.5$. We have checked the possible agreement of our experimental data with the EW growth model. In particular, we have attempted to assess if the square root of the surface roughness scales logarithmically with both growth time and length scale. Although our data could be compatible with this model, the relative large error bars in the film roughness values and the film ultrasmoothness do not allow us to unambiguously identify the growth dynamics of our system as EW. In our case, the film growth dynamics results from the interplay of different growth processes. Thus, as the bias applied is above the physical sputtering threshold and shadowing effects are present, the ions can erode preferably the protruding regions in the growing film surface leading to a surface leveling. In addition, the ion bombardment causes an enhanced surface mobility of the precursor species weakly bound to the film surface. The interplay of these effects would cause a net downhill current of material that tends to smooth the surface profile leading to the observed surface ultrasmoothness.

*Corresponding author. Electronic address: lvb@icmm.csic.es

[1] A. C. Ferrari, Surf. Coat. Technol. **180**, 190 (2004).

[2] A. L. Barabási and H. E. Stanley, *Fractal Concepts in Surface Growth* (Cambridge University Press, Cambridge, 1995).

[3] F. Family and T. Vicsek, J. Phys. A **18**, L75 (1985).

[4] P. Meakin, *Fractals, Scaling and Growth Far from Equilibrium* (Cambridge University Press, Cambridge, 1998).

[5] N. Mutsukura and K. Yoshida, Diamond Relat. Mater. **5**, 919 (1996).

[6] M. Camero, F. J. Gordillo-Vázquez, J. Ortiz, and C. Gómez-Aleixandre, Plasma Sources Sci. Technol. **13**, 121 (2004).

[7] P. Reinke, W. Jacob, and W. Möller, J. Appl. Phys. **74**, 1354 (1993).

[8] M. Weiler, S. Sattel, T. Giessen, K. Jung, H. Ehrhardt, V. S. Veerasamy, and J. Robertson, Phys. Rev. B **53**, 1594 (1996).

[9] M. Siegert, Phys. Rev. E **53**, 3209 (1996).

[10] C. Herring, J. Appl. Phys. **21**, 301 (1950).

[11] C. C. Umbach, R. L. Headrick, and K. C. Chang, Phys. Rev. Lett. **87**, 246104 (2001).

[12] C. Casiraghi, A. C. Ferrari, R. Ohr, A. J. Flewitt, D. P. Chu, and J. Robertson, Phys. Rev. Lett. **91**, 226104 (2003).

[13] M. Moseler, P. Gumbsch, C. Casiraghi, A. C. Ferrari, and J. Robertson, Science **309**, 1545 (2005).

[14] S. F. Edwards and D. R. Wilkinson, Proc. R. Soc. London **381**, 17 (1982).

[15] L. Vázquez, R. C. Salvarezza, and A. J. Arvia, Phys. Rev. Lett. **79**, 709 (1997).

[16] R. C. Salvarezza, L. Vázquez, H. Míguez, R. Mayoral, C. López, and F. Meseguer, Phys. Rev. Lett. **77**, 4572 (1996).

[17] R. Jullien and P. Meakin, Europhys. Lett. **4**, 1385 (1987).

[18] T. S. Cale, V. Mahadev, in *Modeling of Film Deposition for Microelectronic Applications*, Thin Films, Vol. 22, edited by S. Rossnagel and A. Ulman (Academic, San Diego, 1996).

[19] D. Le Bellac, G. A. Niklasson, and C. G. Granqvist, Europhys. Lett. **32**, 155 (1995).

[20] G. T. Dalakos, J. L. Plawsky, and P. D. Persans, Appl. Phys. Lett. **85**, 3462 (2004).

[21] J. H. Jeffries, J. K. Zuo, and M. M. Craig, Phys. Rev. Lett. **76**, 4931 (1996).

[22] C. Riccardi, R. Barni, M. Fontanesi, and P. Tosi, Chem. Phys. Lett. **329**, 66 (2000).

[23] A. von Keudell, Plasma Sources Sci. Technol. **9**, 455 (2000); C. Hopf, W. Jacob, and A. von Keudell, J. Appl. Phys. **97**, 94904 (2005).

[24] Y. Yamashita, K. Katayose, H. Toyoda, and H. Sugai, J. Appl. Phys. **68**, 3735 (1990).

[25] Q. Wei, Z. Y. Pan, Z. J. Li, Z. X. Zhang, L. K. Zang, Y. X. Wang, X. S. Ye, T. Bai, C. Wang, and J. R. Liu, Phys. Rev. B **68**, 235408 (2003).

[26] H. You, Z. Nagy, and K. Huang, Phys. Rev. Lett. **78**, 1367 (1997).

[27] P. Meakin and J. M. Deutch, J. Chem. Phys. **85**, 2320 (1986).

[28] J. T. Drotar, Y.-P. Zhao, T.-M. Lu, and G.-C. Wang, Phys. Rev. B **61**, 3012 (2000).

[29] C. Hopf, A. von Keudell, and W. Jacob, J. Appl. Phys. **94**, 2373 (2003).